Electronic Supplementary Information

Mechanistic insights into electrocatalytically reduced OER performance in marigold-like trimetallic NiFe-based LDH: Charge localisation and d-band orbital filling

Suvankar Deka,[ab] Manju Kumari Jaiswal,[ab] Parasmani Rajput,[cd] Biswajit Choudhury*[ab]

[a]Materials and Energy Laboratory, Physical Sciences Division, Institute of Advanced Study in Science and Technology (IASST), Paschim Boragaon, Vigyan Path, Assam-781035, India

[b]Academy of Scientific and Innovative Research (AcSIR), Ghaziabad- 201002, India

[c]Beamline Development and Application Section, Bhabha Atomic Research Centre, Trombay, Mumbai-400085, India

[d]Homi Bhabha National Institute, Anushakti Nagar, Mumbai-400 094, India

*Email: biswajitchoudhury@iasst.gov.in, biswa.tezu@gmail.com

Section S1

Turn Over Frequency (TOF) Calculation

$TOF = (j \times N_A) / (F \times n \times \Gamma)$ ..... (1)

Where j is current density at a particular overpotential, N_A is Avogadro Number, F is Faraday's constant which is equals to 96485 C mol^{-1}, n is the number of electrons which is equals to 4 for OER, Γ is the surface concentration.

So, first we determined surface concentration of active sites from the redox features of CV.

The calculated area associated with the reduction of Ni^{3+} to Ni^{2+} of NiFe-LDH is 0.000929254 VA

Therefore, the associated charge is = (Calculated area / Scan rate in Vs^{-1})
= 0.000929254 VA / 0.05Vs^{-1} = 0.01859C

Therefore, the number of electron transferred is = 0.01286 C/1.602 $\times 10^{-19}$ C= 1.16012×10^{17}

Since, the reduction of Ni^{3+} to Ni^{2+} is a single electron transfer reaction, the number of electrons calculated above is exactly the same as the number of surface-active sites.

Plugging the above value Γ, and value of j at an overpotential of 100 mV into equation S1 we have,

$TOF = (j \times N_A) / (F \times n \times \Gamma)$
$= (3.09 \times 10^{-3} \times 6.022 \times 10^{23}) / 96485 \times 4 \times 1.16012 \times 10^{17}$
$= 0.042\ sec^{-1}$

Similarly, we have calculated the TOF of NiFe LDH @ 150 mV, 200 mV, 250 mV and 300 mV.

Following the aforementioned procedure, the TOF of ZNF and CNF at different overpotentials (100 mV, 150 mV, 200 mV, 250 mV and 300 mV) has been calculated.

Section S2

Mott−Schottky Analysis

According to Mott−Schottky theory, the space charge capacitance exhibits a dependence on potential given by the equation[1]:

$$\frac{1}{C^2} = \frac{2}{e\varepsilon\varepsilon_0 N_D}\left(E_{applied} - E_{FB} - \frac{KT}{e}\right) \quad \text{..... (2)}$$

where C signifies the capacitance belonging to the space charge region, e indicates the electronic charge (1.602×10^{-19} C), ε being the dielectric constant ($\varepsilon \sim 3.6$)[2], ε_0 is the vacuum permittivity given by 8.854×10^{-14} Fcm^{-1}, $E_{applied,}$ and E_{FB} are the applied and flat band potentials, N_D is carrier concentration (donor density), k and T being the Boltzmann constant and absolute temperature (298 K), respectively. Subsequently, linear fitting of C^{-2} versus V plot yields the slope which is equal to $2/q\varepsilon\varepsilon_0 N_D$. Employing the relation, $N_D = 2/(q\varepsilon\varepsilon_0 \times slope)$ the carrier concentration for NF, ZNF and CNF were determined.

FIGURE FILES

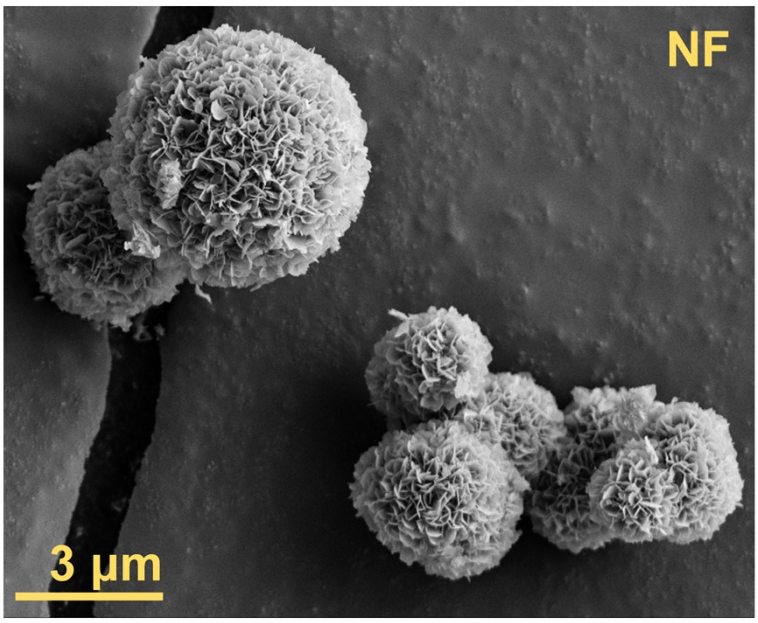

Fig. S1 SEM image of NF.

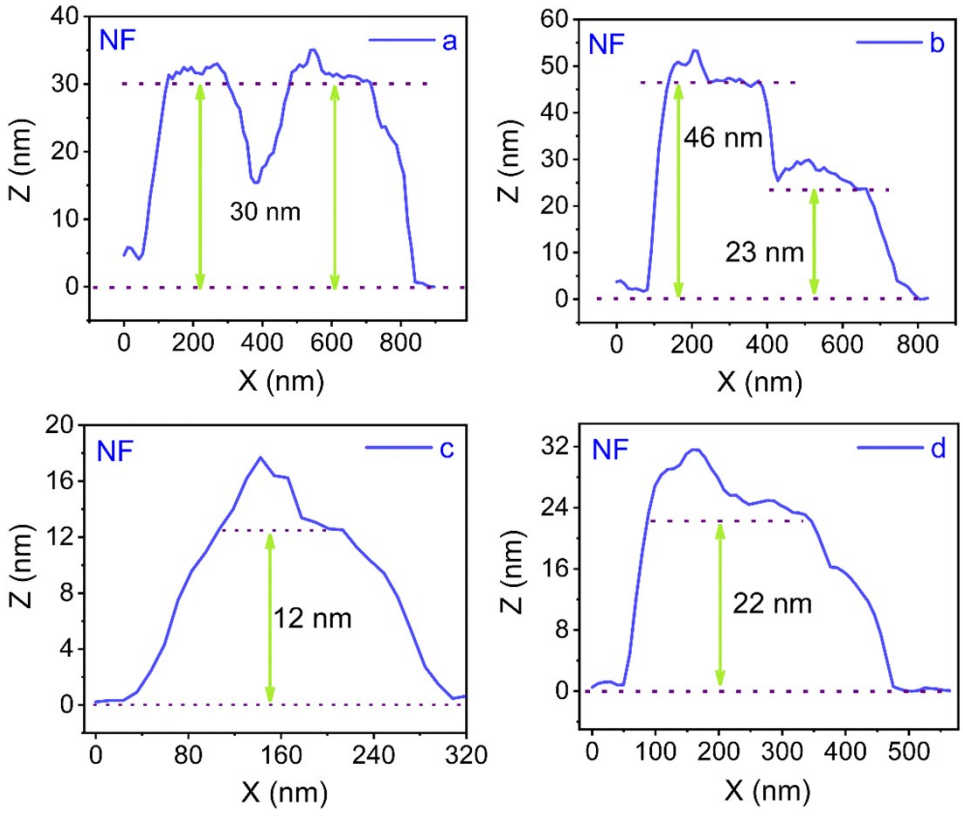

Fig. S2 AFM height profiles of NF.

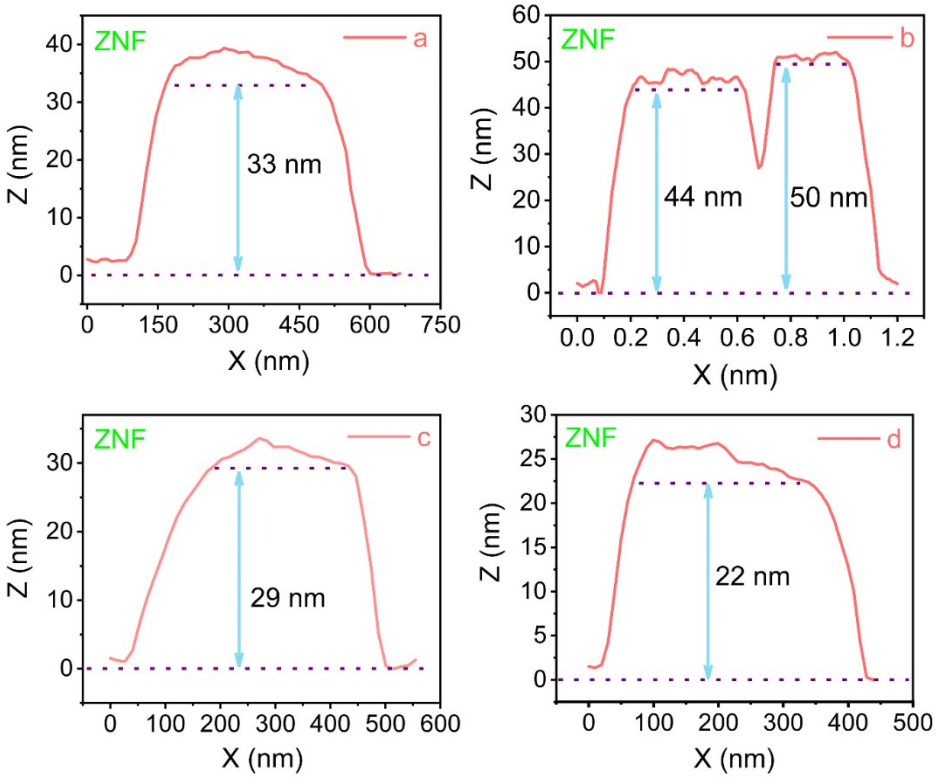

Fig. S3 AFM height profiles of ZNF.

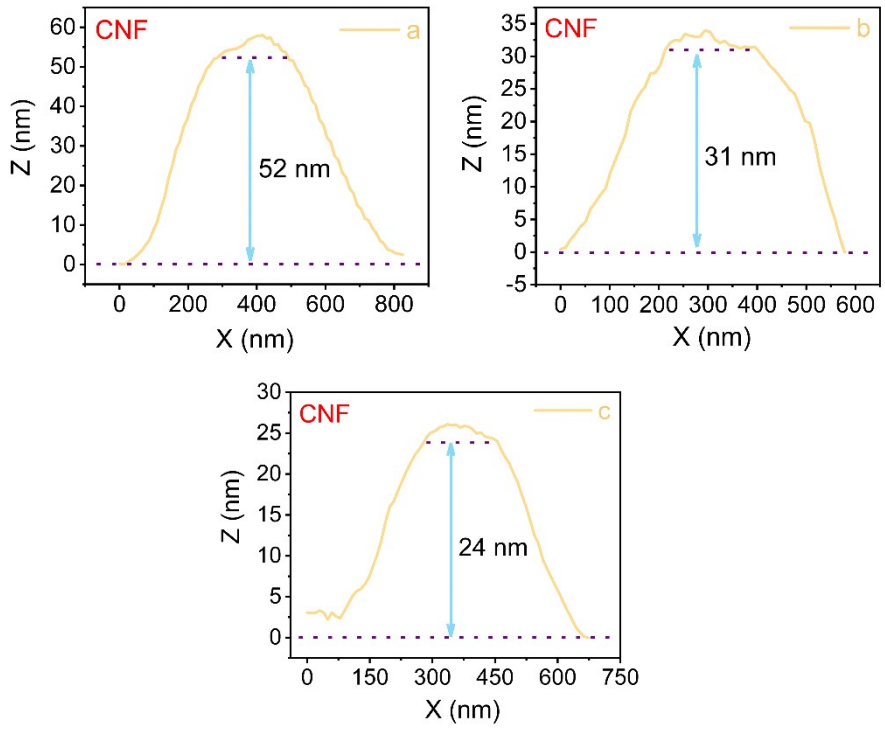

Fig. S4 AFM height profiles of CNF.

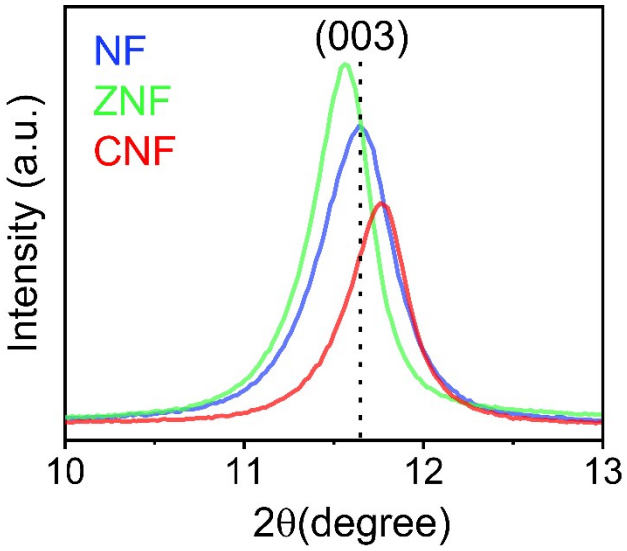

Fig. S5 XRD pattern of NF, ZNF, and CNF showing sifting of (003) plane.

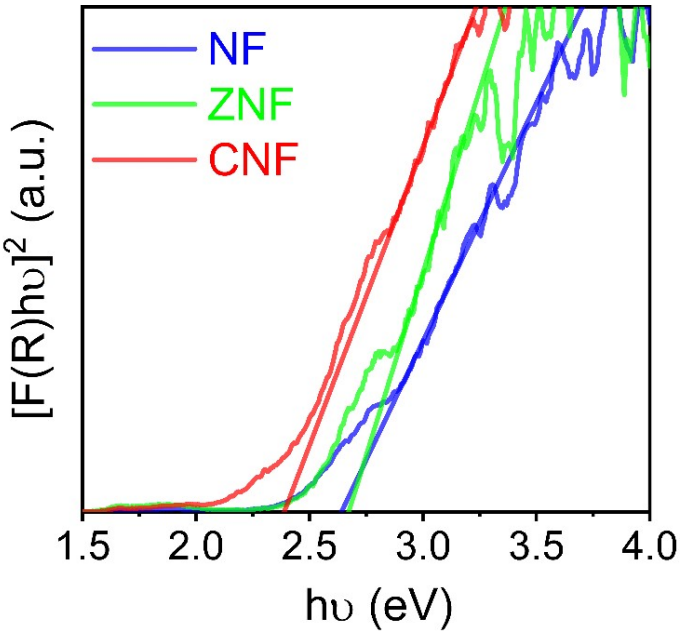

Fig. S6 Tauc's plot of as-synthesized NF, ZNF, and CNF.

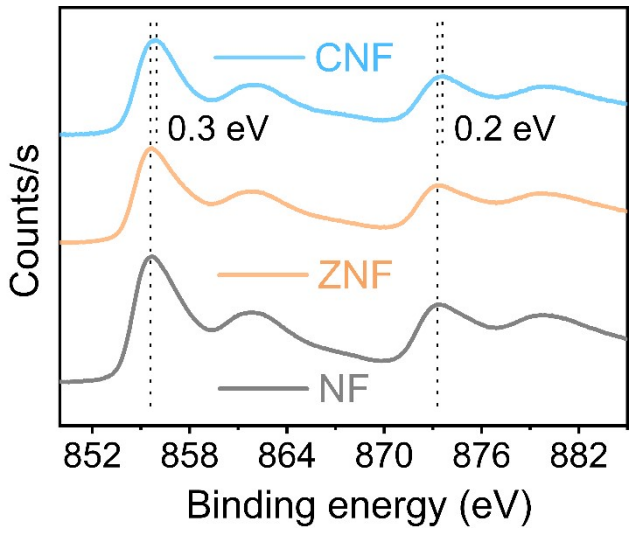

Fig. S7 Ni 2p Spectra for NF, ZNF, and CNF.

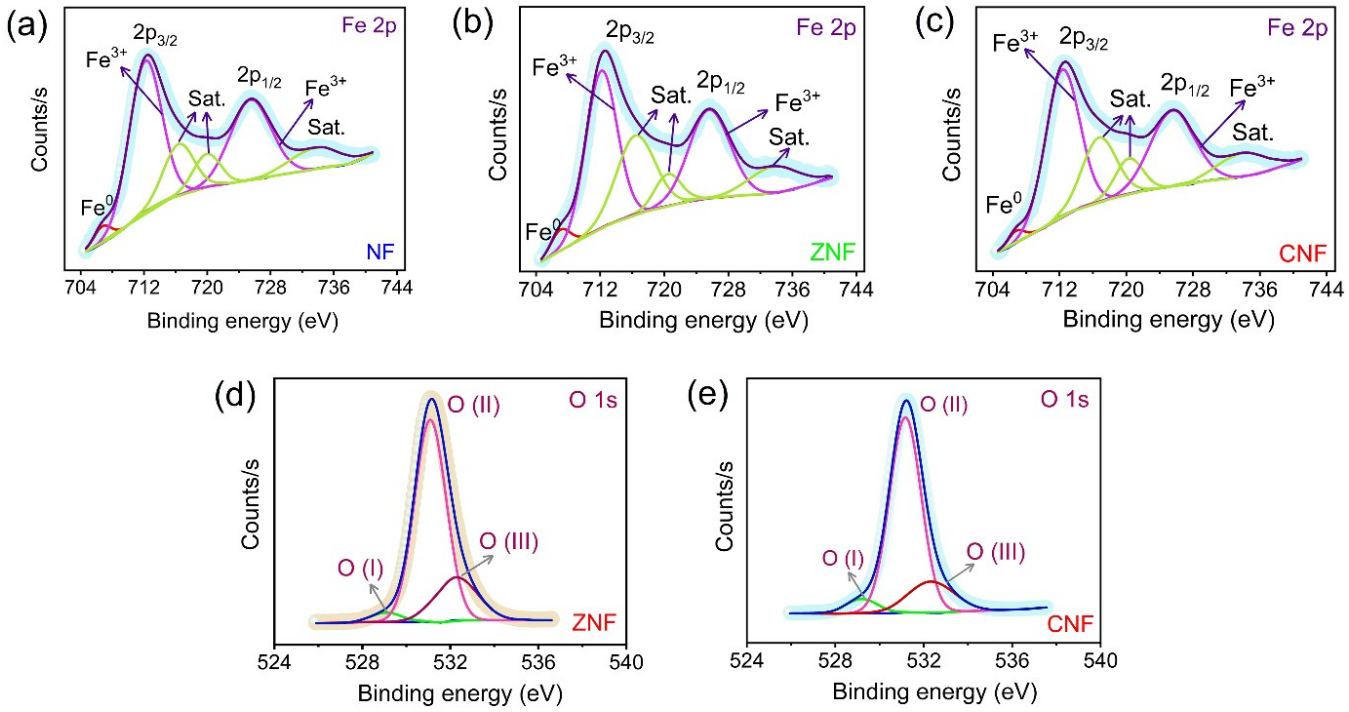

Fig. S8 XPS plots of (a-c) Fe 2p spectrum for NF, ZNF, and CNF (d,e) O 1s spectrum for ZNF and CNF

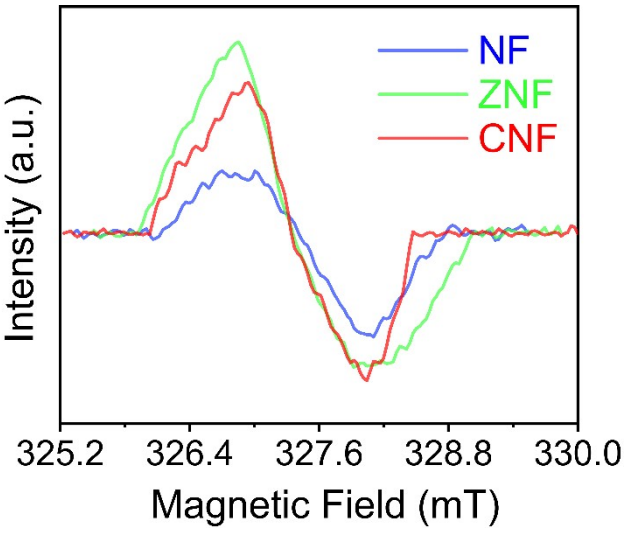

Fig. S9 EPR spectra of NF, ZNF, and CNF

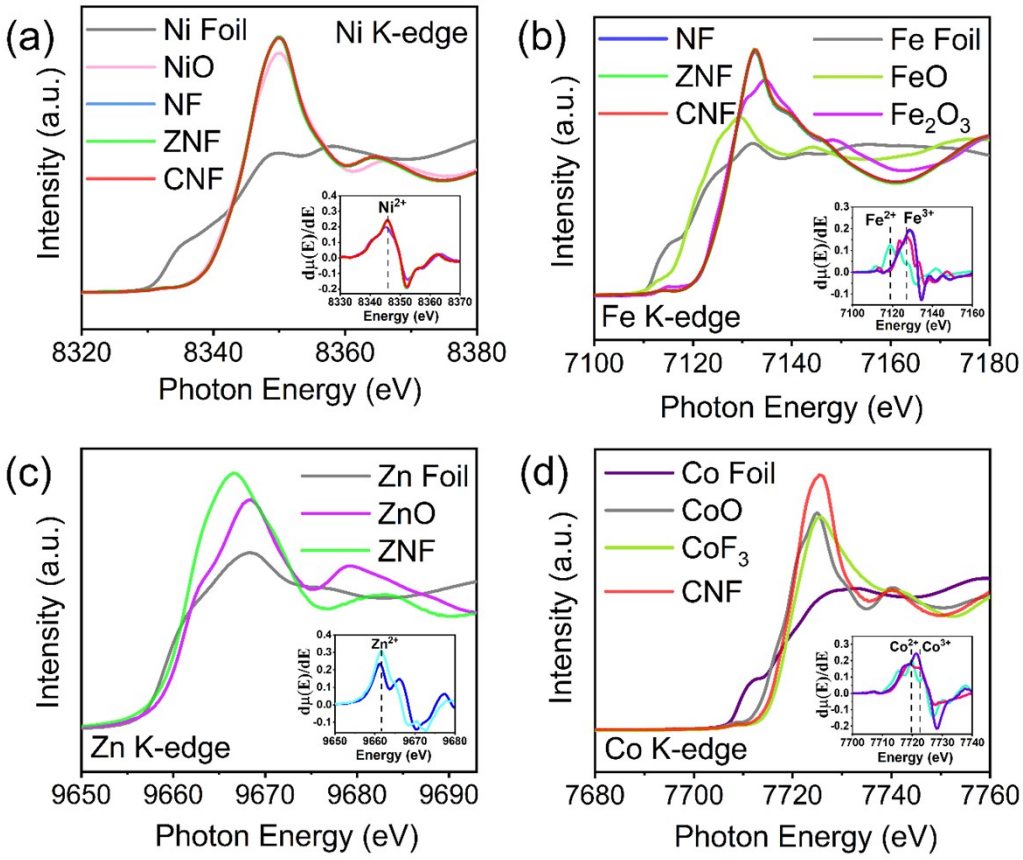

Fig. S10 XANES spectra of (a) Ni K-edge for NF, ZNF, and CNF (b) Fe K-edge for NF, ZNF and CNF. (c) Zn K-edge for ZNF. (d) Co K-edge for CNF along with references Ni foil, NiO, Fe foil, FeO, Fe_2O_3, Zn foil, ZnO, Co foil, CoO, and CoF_3. The first derivate spectra of Ni K-edge, Fe K-edge, Zn K-edge, and Co K-edge have been shown as inset in their corresponding XANES spectra.

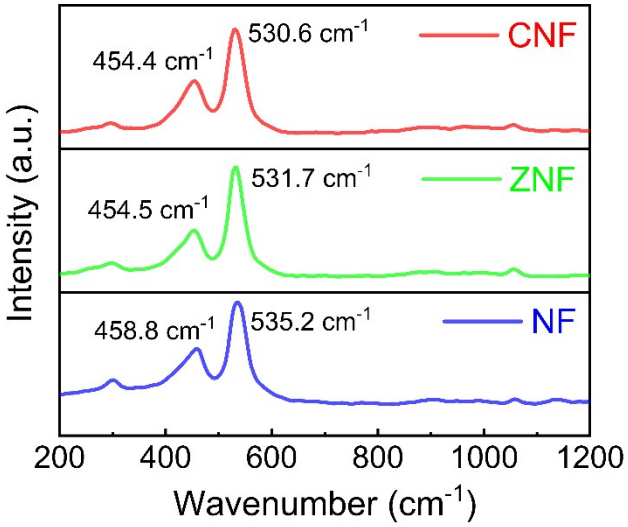

Fig. S11 Raman Profiles of NF, ZNF, and CNF within a scope of 200 cm^{-1} – 1200 cm^{-1}.

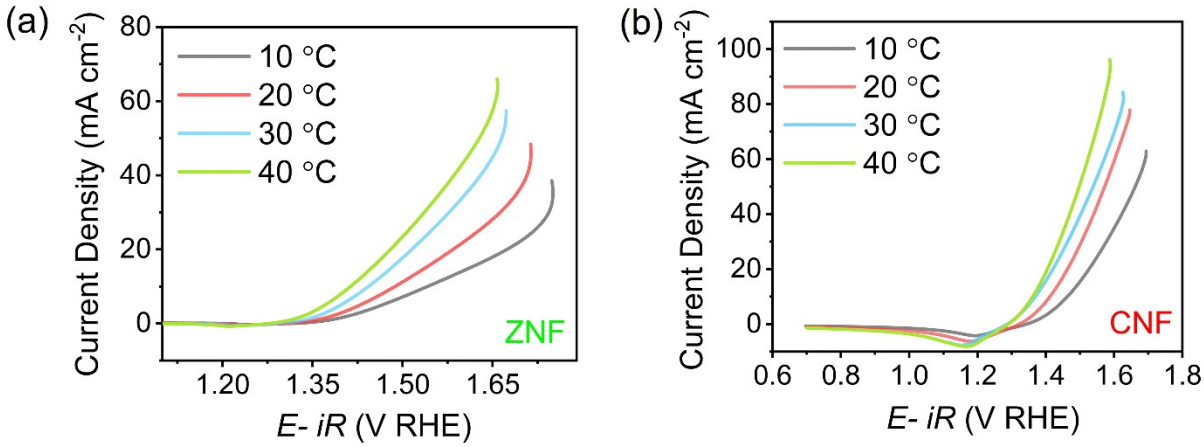

Fig. S12 Polarization curves of (a) ZNF and (b) CNF at temperatures ranging from (10 °C to 40 °C)

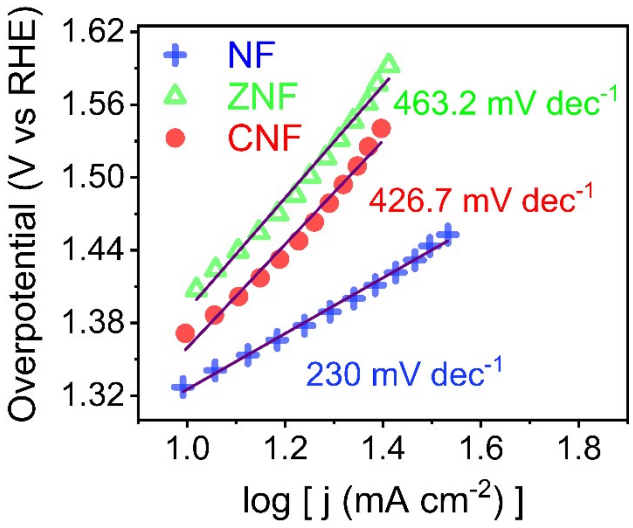

Fig. S13 Tafel plots of NF, ZNF, and CNF obtained from chronoamperometric measurements with *iR*-corrected overpotential.

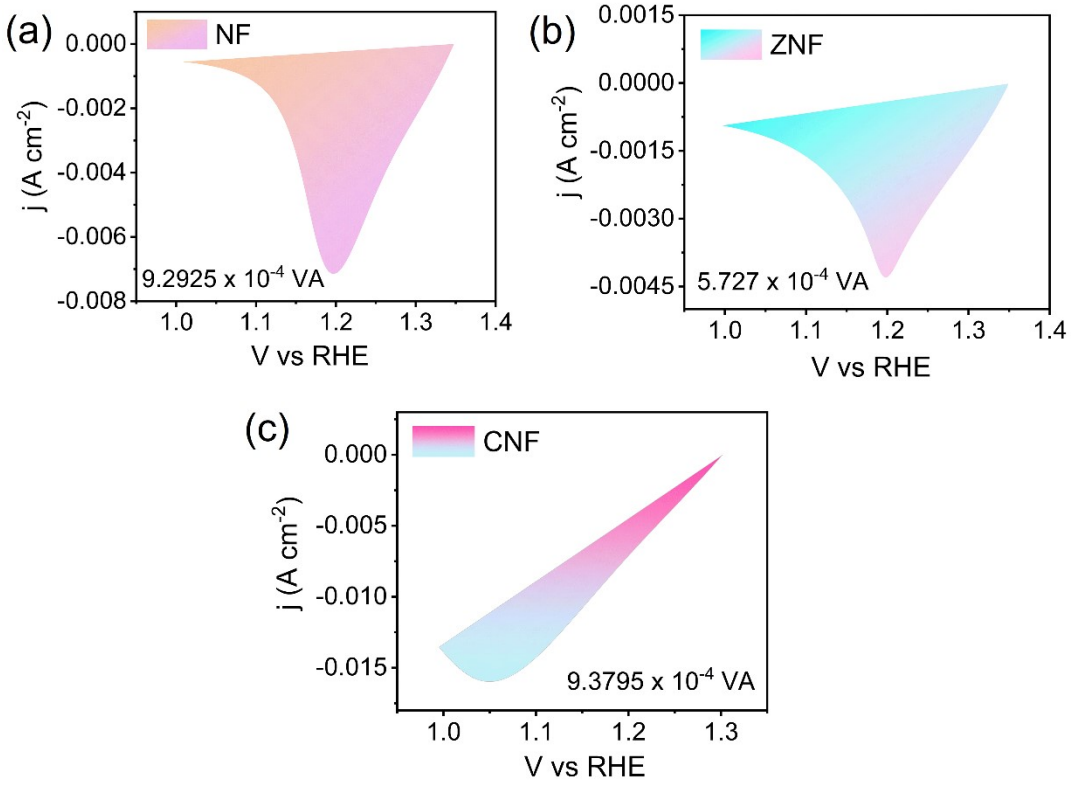

Fig. S14 Reduction surface area of (a) NF (b) ZNF and (c) CNF for calculating TOF. (turn-over frequency)

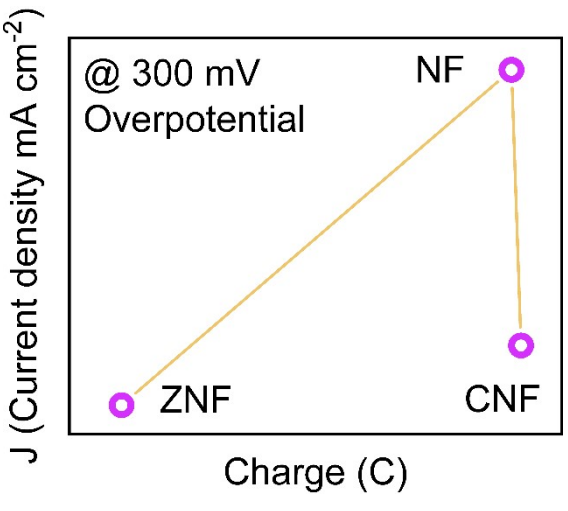

Fig. S15 Accumulation of charge over the catalyst surface vs current density at a potential of 1.53 V vs RHE.

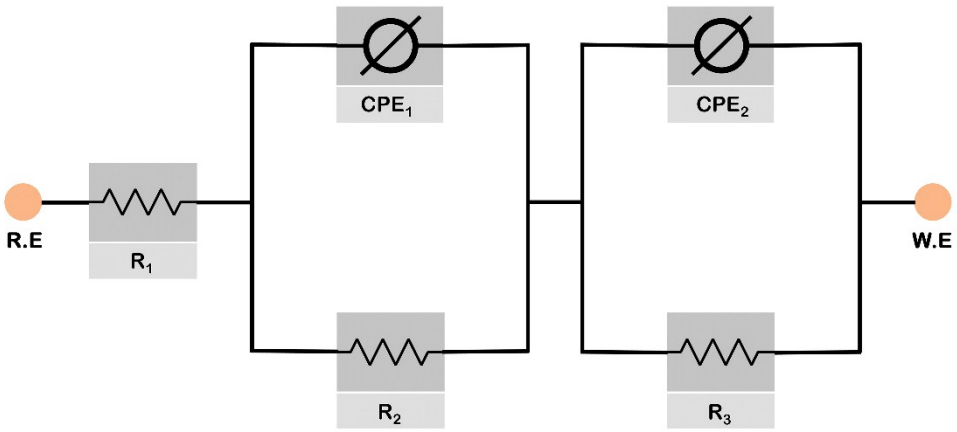

Fig. S16 Modified Randels equivalent electrical circuit model (2R CPE) for fitting EIS data.

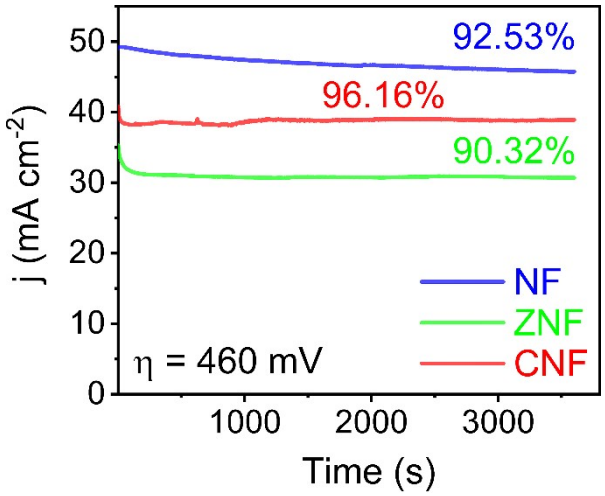

Fig. S17 Chronoamperometric curves of NF, ZNF, and CNF recorded at an overpotential of 460 mV without iR Correction.

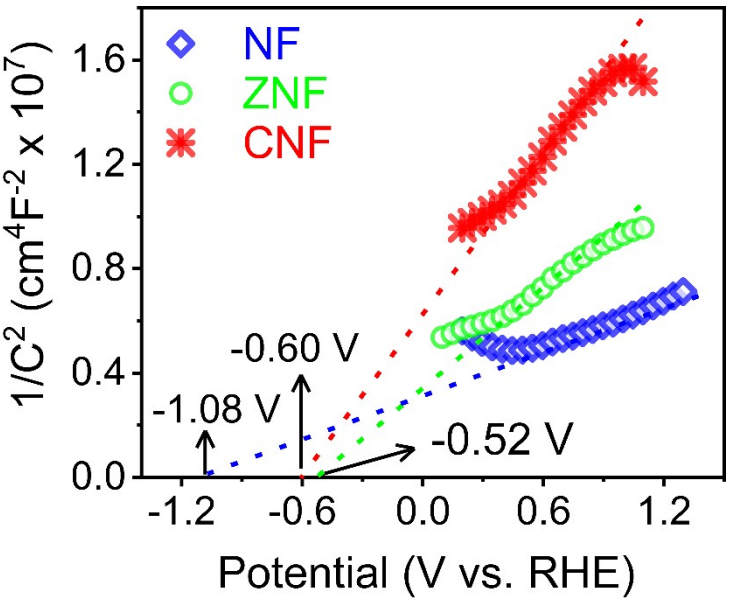

Fig. S18 Mott-Schottky Plot for NF, ZNF and CNF.

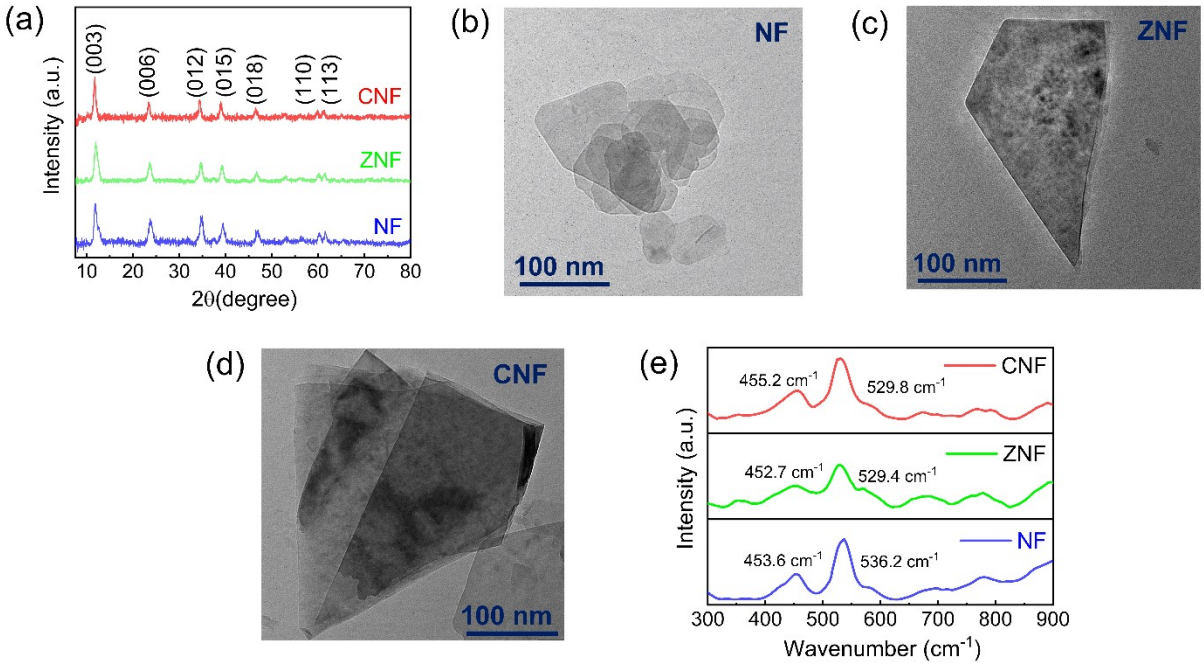

Fig S19. Post characterization (a) XRD patterns, (b-d) TEM images of NF, ZNF, and CNF (e) Raman profile of NF, ZNF, and CNF.

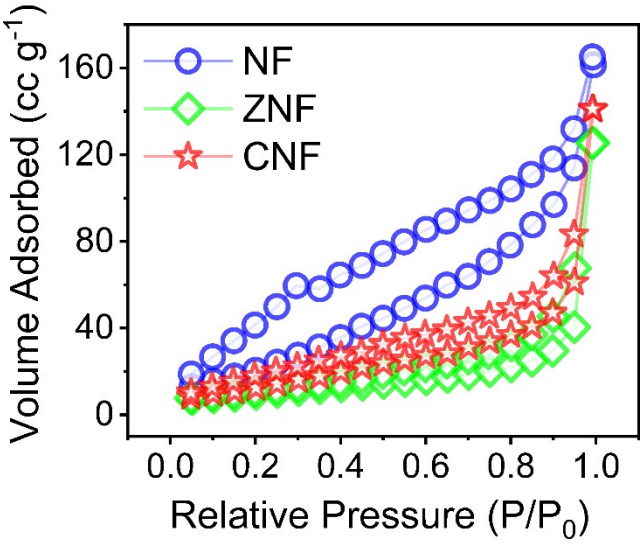

Fig. S20 Nitrogen adsorption/desorption isotherm

TABLES

Table S1 XPS fitting parameters for the binding energies of the as-prepared catalysts.

Catalyst	**Peak position (eV)**											
	Ni^{2+}		Ni^{3+}		Fe^{3+}		Zn^{2+}		Co^{2+}		Co^{3+}	
	$2p_{3/2}$	$2p_{1/2}$	$2p_{3/2}$	$2p_{1/2}$	$2p_{3/2}$	$2p_{1/2}$	$2p_{3/2}$	$2p_{1/2}$	$2p_{3/2}$	$2p_{1/2}$	$2p_{3/2}$	$2p_{1/2}$
NF	855.2	872.8	856.6	874.3	712.2	725.5	-	-	-	-	-	-
ZNF	855.3	872.9	856.7	874.5	711.9	725.6	1021.3	1044.4	-	-	-	-
CNF	855.4	873.1	856.6	874.9	712.3	725.5	-	-	781.9	797.4	780.5	796.3

Table S2 XPS deconvoluted peak positions of O1s Spectra of NF, ZNF and CNF.

Catalyst	**Peak position (eV)**			**Constituents (%)**		
	O (I)	O (II)	O (III)	O (I)	O (II)	O (III)
NF	528.9	531.0	532.3	5.43	77.56	17.01

ZNF	529.1	531.1	532.2	3.38	75.10	21.51
CNF	529.2	531.1	532.3	5.69	76.69	17.62

Table S3 Structural parameters were obtained by fitting the experimental XAFS data at the Ni K-edge. The CN is the coordination number, R is the interatomic distance, and σ^2 is the Debye-Waller factor. The numbers in parentheses indicate the uncertainty in the last digit.

Sample	Path	CN	R(Å)	σ^2 (Å^2)	R-factor
NF	Ni-O	5.6 (2)	2.053 (2)	0.0047 (2)	0.014
	Ni-Ni	5.9 (3)	3.095 (3)	0.0048 (3)	
ZNF	Ni-O	5.5 (2)	2.055 (3)	0.0048(3)	0.013
	Ni-Ni	5.6 (3)	3.107 (3)	0.0051(4)	
CNF	Ni-O	5.5 (2)	2.039 (3)	0.0049(2)	0.013
	Ni-Ni	5.8 (3)	3.111 (3)	0.0052(4)	

Table S4 Structural parameters were obtained by fitting the experimental XAFS data at the Fe K-edge. The CN is the coordination number, R is the interatomic distance, and σ^2 is the Debye-Waller factor. The numbers in parentheses indicate the uncertainty in the last digit.

Sample	Path	CN	R(Å)	σ^2 (Å^2)	R-factor
NF	Fe-O	5.5 (2)	2.010 (2)	0.0049 (3)	0.011
	Fe-Fe	5.8 (3)	3.097(3)	0.0053 (3)	
ZNF	Fe-O	5.5 (2)	2.011(2)	0.0049(3)	0.012
	Fe-Fe	5.5 (3)	3.099(4)	0.0051(4)	
CNF	Fe-O	5.4 (2)	2.012(3)	0.0049(3)	0.011
	Fe-Fe	5.7 (3)	3.099(3)	0.0053(4)	

Table S5 Structural parameters were obtained by fitting the experimental XAFS data at the Zn K-edge. The CN is the coordination number, R is the interatomic distance, and σ^2 is the Debye-Waller factor. The numbers in parentheses indicate the uncertainty in the last digit.

Sample	Path	CN	R(Å)	σ^2 (Å^2)	R-factor
ZNF	Zn-O	4.9 (2)	2.055 (2)	0.0065 (3)	0.013
	Zn-Zn	4.7 (3)	3.143 (3)	0.0065 (3)	

Table S6. Structural parameters were obtained by fitting the experimental XAFS data at the Co K-edge. The CN is the coordination number, R is the interatomic distance, and σ^2 is the Debye-Waller factor. The numbers in parentheses indicate the uncertainty in the last digit.

Sample	Path	CN	R(Å)	σ^2 (Å^2)	R-factor
CNF	Co-O	5.1 (2)	2.062 (3)	0.0055 (3)	0.013
	Co-Co	5.6 (3)	3.109 (3)	0.0054 (4)	

Table S7 Overpotential, Tafel constant, and Tafel slope values of NF, ZNF, and CNF at different temperatures.

Sample	Temperature	Overpotential at 10 mA cm^{-2} (mV)	Tafel Constant (mV)	Tafel Slope at region A (mV/dec) Region A	Tafel Slope at region B (mV/dec) Region B
NF	10	180	105	40.9	144.6
	20	150	89	36.4	120.2
	30	130	73	32.5	113.6
	40	100	56.9	27.3	80.7
ZNF	10	313	154	76.2	376.0
	20	260	129	60.0	271.0

	30	213	109	54.7	225.9
	40	185	85	53.9	197.7
CNF	10	233.2	137.8	63.1	194.4
	20	184.2	109.3	54.1	163.4
	30	140.5	72.9	51.2	157.1
	40	132.5	70.3	43.0	133.6

Table S8 Steady-State current measured from chronoamperometric curves for NF at various overpotentials.

NF		**ZNF**		**CNF**	
Potential (V)	Current (mA) measured from CA	Potential (V)	Current (mA) measured from CA	Potential (V)	Current (mA) measured from CA
0.47	9.81	0.55	10.45	0.51	9.92
0.49	11.41	0.57	11.44	0.53	11.37
0.51	13.31	0.59	12.72	0.55	12.75

0.53	15.28	0.61	14.02	0.57	14.10
0.55	17.37	0.63	15.34	0.59	15.46
0.57	19.58	0.65	16.64	0.61	16.91
0.59	21.92	0.67	17.85	0.63	18.20
0.61	24.23	0.69	19.21	0.65	19.52
0.63	26.69	0.71	20.47	0.67	20.86
0.65	29.21	0.73	21.84	0.69	22.27
0.67	31.36	0.75	23.33	0.71	23.47
0.69	34.10	0.77	24.48	0.73	24.93

Table S9 Comparison table for various state-of-art electrocatalysts for OER.

Catalyst	Substrate / Electrolyte	Overpotential (mV)	Tafel Slope	C_{dl} (mF	TOF (s^{-1})	Ref.

		@ 10 mA cm^{-2}	(mV dec^{-1})	cm^{-2})		
NiFe LDH	CC/1 M KOH	134.0	101.7	1.62	1.12	Our work
NiFe LDH	CC/1 M MOH	295.0	260.0	-	0.092	[3]
NiFe LDH	NF/1M KOH	320.0	37.0	1.08	-	[4]
Ce@NiFe LDH	NF/1M KOH	205.0	40.1	1.52	0.084	[5]
$Ni_3Fe_{0.5}V_{0.5}$ (oxy)hydroxide	CFP/1M KOH	200.0	39.0	-	0.574	[6]
ZnNiFe LDH	1 M KOH	240.0	273.7	1.09	0.35	Our work
NiFe LDH/ZnO	NF/1M KOH	210.0	63.0	1.1	-	[7]
ZnNiFe LDH	1M KOH	470.0	86.0	0.0003	-	[8]
CoNiFe LDH	1 M KOH	160.0	162.0	1.09	0.37	Our work
NiFeCo-LDH	GCE/ 1M KOH	319.0	81.0	0.28	-	[9]
NiCoFe LDH	CFP/1M NaOH	288.0	92.0	2.62	-	[10]
CoFe@NiFe-200	NF/1M KOH	190.0	45.7	-	0.011	[11]
CoNiFe LDH/$RuO_{2.1}$	GC/1M KOH	332.0	48.9	-	0.045	[12]

Table S10 Surface Area, Pore Size, and Pore Volume obtained from nitrogen adsorption-desorption isotherms

Sample	BET Surface Area ($m^2\ g^{-1}$)	Pore Size (Å)	Pore Volume (cc g^{-1})
NF	103.09	17.05	0.249
ZNF	34.49	15.33	0.194
CNF	56.85	15.30	0.218

Table S11 Calculated FWHM values from Raman profile after electrochemical measurement

Sample	FWHM (cm^{-1})
NF	33.59
ZNF	37.57
CNF	34.30

References

1 M. K. Jaiswal and B. Choudhury, *ACS Appl. Nano Mater.*, 2022, **5**, 3599–3610.

2 Y. Lu, P. Yang, Y. Li, D. Wen, J. Luo, S. Wang, F. Wu, L. Fang and Y. Pang, *Molecules*, **2021**, *26* (16).

3 K. Bera, R. Madhu, H. N. Dhandapani, S. Nagappan, A. De and S. Kundu, *Inorg. Chem.*, 2022, **61**, 16895–16904.

4 K. B. Ibrahim, W. N. Su, M. C. Tsai, A. W. Kahsay, S. A. Chala, M. K. Birhanu, J. F. Lee and B. J. Hwang, *Mater. Today Chem.*, 2022, **24**, 100824.

5 M. Liu, K. A. Min, B. Han and L. Y. S. Lee, *Adv. Energy Mater.*, 2021, **11**, 2101281.

6 J. Jiang, F. Sun, S. Zhou, W. Hu, H. Zhang, J. Dong, Z. Jiang, J. Zhao, J. Li, W. Yan and M. Wang, *Nat. Commun.,* 2018, **9**, 1–12.

7 Y. Luo, Y. Wu, D. Wu, C. Huang, D. Xiao, H. Chen, S. Zheng and P. K. Chu, *ACS Appl. Mater. Interfaces*, 2020, **12**, 42850–42858.

8 J. Xie, J. Xin, R. Wang, X. Zhang, F. Lei, H. Qu, P. Hao, G. Cui, B. Tang and Y. Xie, *Nano Energy*, 2018, **53**, 74–82.

9 Y. Lin, H. Wang, C.-K. Peng, L. Bu, C.-L. Chiang, K. Tian, Y. Zhao, J. Zhao, Y.-G. Lin, J.-M. Lee, L. Gao, Y. Lin, L. Bu, K. Tian, Y. Zhao, J. Zhao, L. Gao, H. Wang, J. Lee, C. Peng and C. Chiang, *Small*, 2020, **16**, 2002426.

10 M. Zhang, Y. Liu, B. Liu, Z. Chen, H. Xu and K. Yan, *ACS Catal.*, 2020, **10**, 5179–5189.

11 R. Yang, Y. Zhou, Y. Xing, D. Li, D. Jiang, M. Chen, W. Shi and S. Yuan, *Appl. Catal. B*, 2019, **253**, 131–139.

12 X. Lu, N. Sakai, D. Tang, X. Li, T. Taniguchi, R. Ma and T. Sasaki, *ACS Appl. Mater. Interfaces*, 2020, **12**, 33083–33093.